Jurnal Teknologi

Full paper

# Numerical Analysis on the CO-NO Formation Production near Burner Throat in Swirling Flow Combustion System

Mohamad Shaiful Ashrul Ishak[a,b*], Mohammad Nazri Mohd Jaafar[b]

[a]*School of Manufacturing Engineering, Universiti Malaysia Perlis,P.O Box 77, Pejabat Pos Besar, 01000 Kangar, Perlis, Malaysia*
[b]*Department of Aeronautics, Automotive & Ocean Engineering, Faculty of Mechanical Engineering,Universiti Teknologi Malaysia, 81310 UTM Johor Bahru, Johor, Malaysia*

*Corresponding author: mshaiful@unimap.edu.my

**Article history**

Received :1 January 2014
Received in revised form :
15 February 2014
Accepted :18 March 2014

**Graphical abstract**

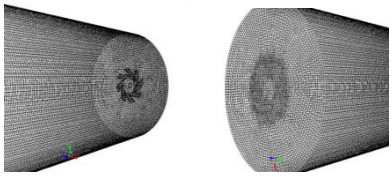

**Abstract**

The main purpose of this paper is to study the Computational Fluid Dynamics (CFD) prediction on CO-NO formation production inside the combustor close to burner throat while varying the swirl angle of the radial swirler. Air swirler adds sufficient swirling to the inlet flow to generate central recirculation region (CRZ) which is necessary for flame stability and fuel air mixing enhancement. Therefore, designing an appropriate air swirler is a challenge to produce stable, efficient and low emission combustion with low pressure losses. A liquid fuel burner system with different radial air swirler with 280 mm inside diameter combustor of 1000 mm length has been investigated. Analysis were carried out using four different radial air swirlers having 30°, 40°, 50° and 60° vane angles. The flow behavior was investigated numerically using CFD solver Ansys Fluent. This study has provided characteristic insight into the formation and production of CO and pollutant NO inside the combustion chamber. Results show that the swirling action is augmented with the increase in the swirl angle, which leads to increase in the center core reverse flow, therefore reducing the CO and pollutant NO formation. The outcome of this work will help in finding out the optimum swirling angle which will lead to less emission.

*Keywords*: Swirler; combustor; carbon monoxide; pollutant NO; CFD simulation



## 1.0 INTRODUCTION

Swirling jets are used for the stabilisation and control of a flame and to achieve a high intensity of combustion. The common method of generating swirl is by using angle vanes in the passages of air. The characteristic of the swirling jet depends on the swirler vane angle [1]. Various investigation on the effects of swirl on the flame stability for swirl flame in the unconfined space have shown increasing fuel/air mixing as the degree of swirl increased [2]. The size and strength of the central recirculation zone (CRZ) also increased with an increase in swirl intensity. At low flow rates or swirl numbers, long yellow and highly luminous flames are produced indicating poor fuel-air mixing [3]. However, when the swirl number is increased, the CRZ increases in size, initially in width until restricted by the diameter of the combustor and then begin to increase in length [3]. Measurements of the flame length and stabilization distance carried out in the series of butane-propane-air flames with swirl, have shown that both decrease markedly with increasing degree of swirl [4]. Tian on the other hand, numerically compared the effects of swirling and non-swirling system on combustion [5]. He demonstrated that the existence of swirl helps improve combustion efficiency, decreases all pollutants and increases flame temperature. He also observed that during the presence of a swirl, a shorter blue flame was observed indicating a short time for peak temperature resulting in good mixing while non-swirling system showed a longer yellow flame indicating a long time peak temperature, and there is still some fuel left un-vaporised. Increasing of swirl number improves the flame stability due to the presence of the recirculation zone [6]. Increasing the swirl number will increase the angle of the jet thereby increasing the total available surface area per unit volume of the jet. This allows further mixing with the surrounding fluid in the free jet and the central core of the flow [7]. It has also been shown that flames with low swirl have instability problems, because of the absence of the recirculation zone [8].

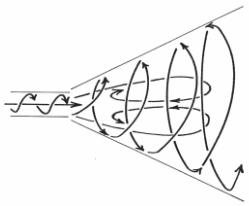

**Figure 1** Jet flow of high degree of swirl (S > 0.6) resulting in significant lateral as well as longitudinal pressure gradients. Compared to its non-swirling counterpart, the jet is much wider, slower and there exist a central toroidal recirculation zone [8]

Figure 1 shows schematically a jet flow with high degree of swirl, which results in significant lateral as well as longitudinal pressure gradients. Compared to its non-swirling counterpart, the jet is much wider, slower and with a central toroidal recirculation zone. In combustion, the presence of this recirculation zone plays an important role in flame stabilization by providing a rearward hot flow of combustion products at the centre of the combustion chamber which is a reduced velocity region where flame speed and flow velocity can be matched. Swirls also act to shorten the flame length and this is advantageous for having more compact burner design [9].

The degree of swirl in the flow is quantified by dimensionless parameter, S known as swirl number which is defined as [10];

$$S = \frac{G_\phi}{G_\chi . r_o} \tag{1}$$

where $G_\phi$ is the axial flux of angular momentum:

$$G_\phi = 2\pi \int_0^\infty \rho U_x U_\theta r^2 dr \tag{2}$$

and $G_x$ is the axial flux of axial momentum (axial thrust):

$$G_\chi = 2\pi \int_0^\infty \rho U_x^2 r dr + 2\pi \int_0^\infty p r dr \tag{3}$$

In the above, $r_o$ is the outer radius of the swirler and $U_x$ and $U_\theta$ are the axial and tangential component of velocity at radius $r$.

Since the pressure term in Equation (3) is difficult to calculate due to the fact that pressure varies with position in the swirling jet, the above definition for swirl number can be simplified by omitting this pressure term. Swirl number can be redefined as:

$$S' = \frac{G_\phi}{G_x' r_o} \tag{4}$$

Where

$$G_x' = 2\pi \int_0^\infty \rho U^2{}_x r dr \tag{5}$$

The swirl number should, if possible, be determined from measured values of velocity and static pressure profiles. However, this is frequently not possible due to the lack of detailed experimental results. Therefore, it has been shown that the swirl number may be satisfactorily calculated from geometry of most swirl generator [10].

The main focus of this research is to investigate the effect of varying the swirl angle on formations of Carbon monoxide (CO) and pollutant nitrogen oxide (NO) close to the burner throat inside the combustor.

In this paper, flow pattern characteristics including the temperature profile, CO and pollutant NO distribution, which are the main characteristics of the swirling flows, are studied to understand the physical processes by modelling the flow using Ansys CFD software.

## ■2.0 MODELING, MESHING AND BOUNDARY CONDITION

The basic geometry of the gas turbine can combustor is shown in Figure 2 and Figure 3. The size of the combustor is 1000 mm in the Z direction, 280 mm in the X and Y direction. The primary inlet air is guided by radial curve vanes swirler to give the air a swirling velocity component. Standard Ansys database of liquid diesel ($C_{10}H_{22}$) is injected at the center of swirler. The transverse analysis is focused downstream of the swirler in the expansion chamber at various cross section stations (z/D = 0.2 to 1.0) as shown in Figure 3. Four different vane angles of 30°, 40°, 50° and 60° were analyzed numerically at different boundary conditions to show the effects of the swirler configurations on the turbulence production, recirculation zone and also pressure loss. The intake condition for the combustion simulation is at stoichiometry. The technical data of the four swirlers used in this study are listed in Table 1.

The physical domains of the radial swirlers were decomposed to several volumes to facilitate meshing with cooper hexahedral structured grid. The geometry meshing was done to have a variable density distribution by mean of small mesh size which was incorporated in high gradient zone and bigger size in low gradient zone. The combustor model meshing for the present work is shown in Figure 4. The resulting base mesh is contains approximately 0.6 million cells, which were then applied in this simulation work and presented in this paper.

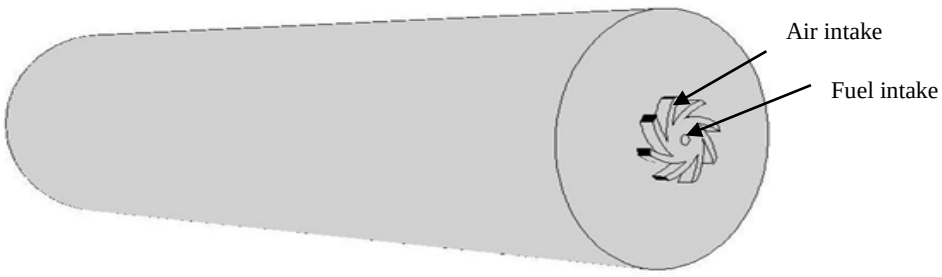


**Figure 2** Combustor model

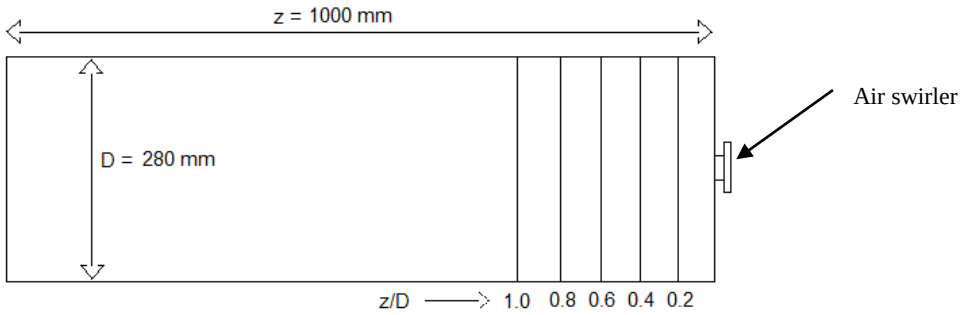


**Figure 3** Details of position of transvers measuring stations indicated by cross section lines (z/D = 0.2 to 1.0) from the swirler throat

**Table 1** Technical data of the swirlers

| | | | | |
|---|---|---|---|---|
| Swirler angle | 30° | 40° | 50° | 60° |
| Swirl No. (S) | 0.366 | 0.630 | 0.978 | 1.427 |
| Passage width, *h* (mm) | 13.6 | 12.3 | 11.2 | 9.6 |
| Hub diameter, *d* (mm) | 50 | | | |
| Outer diameter, *D* (mm) | 98 | | | |

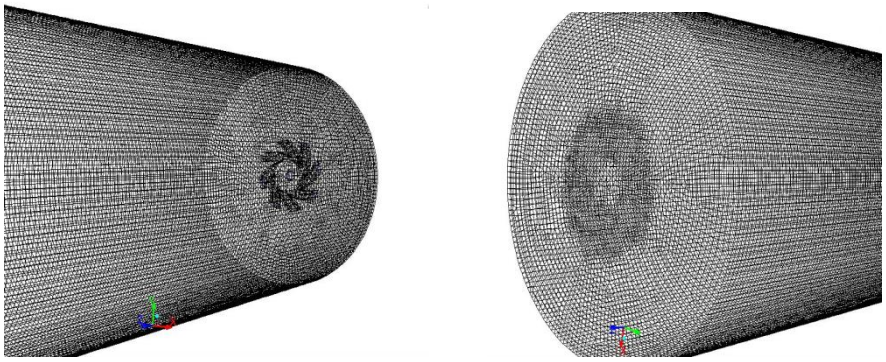

**Figure 4** Combustor model meshing

In the present simulation, k-epsilon turbulence model was used. Turbulence is represented by the realizable k-epsilon model, which provides an optimal choice and economy for internal turbulent flows [11]. The boundary conditions for this simulation are the inlet, standard wall function and the outlet as the boundaries. At the inlet of the computational region, the inlet boundary condition is defined as mass flow inlet for air supply and fuel nozzle while the exit boundary is defined as outflow. Some assumptions for boundary conditions that were not directly measured had to be made as follows:

i. Velocity components and turbulence quantities at the inlet were constant throughout the cross section;
ii. Turbulence at inlet is calculated from the following equations [12]:

$$k_{inlet} = 0.002(u^2)_{inlet} \quad (6)$$

$$\varepsilon = \frac{k_{inlet}^{1.5}}{0.3D} \quad (7)$$

where, u is the axial inlet flow velocity and *D* is the hydraulic diameter.

A collection of physical models was used to simulate the turbulent liquid fuel reacting flows. These models were selected due to their robustness and accuracy for industrial applications.

*Turbulence Model:* The current study uses the realizable *k–ε* turbulence model. This model is in the class of two-equation models in which the solution of two separate transport equations allows the turbulent velocity and length scales to be independently determined. The realizable *k–ε* turbulence model is robust, economic and reasonably accurate over a wide range of turbulent flow. The realizable *k–ε* turbulence model solves transport equations for kinetic energy (*k*) and its dissipation rate (*ε*). It assumes that the flow is fully turbulent, and the effects of molecular viscosity are negligible. The realizable *k–ε* turbulence

model is therefore valid for fully turbulent flows, consistent with the flow characteristics in a typical combustion chamber.

*Combustion Models:* Combustion models are characterized by the type of mixing (e.g. non-premixed, premixed or partially premixed) and the reaction chemistry (e.g. finite-rate chemistry or fast chemistry). Liquid fuel combustion primarily takes place in a diffusion-limited mode (non-premixed) where fuel and oxidant are brought into contact via mixing and then react. In these types of flames, it can generally be assumed that the turbulent mixing rate is much slower than the chemical kinetics rates (fast chemistry), and hence, will be the rate-limiting step. The current study used the eddy-dissipation combustion model, which assumed that the reaction rate is controlled by the turbulent mixing rate. Hence, the turbulent mixing rate in conjunction with a global reaction mechanism is used to predict local temperatures and species profiles. This model solves the conservation equations describing convection, diffusion, and reaction sources for each component species.

*NO*x *Formation Models:* The NOx formations models used in this study include the primary NOx formation mechanisms, i.e. thermal, prompt, and fuel [13]. For thermal and prompt NOx, only the transport equation of NO is solved

$$\frac{\partial}{\partial t}(\rho Y_{NO}) + \Delta \cdot (\rho \vec{v} Y_{NO}) = \Delta \cdot (\rho D \Delta Y_{NO}) + S_{NO} \quad (8)$$

These transport equations are solved based on the given flow field and combustion solution. In other words, NOx is post-processed from the combustion simulation. The formation of thermal NOx is then determined by the extended Zeldovich mechanism and the rate constants for the mechanism are measured from experiments [14]. The current study also applied partial equilibrium model to predict O atom concentrations and assumed lean fuel conditions for OH predictions. The prompt NOx formation depends on local fuel-to-air ratio and carbon numbers. The rate constants in the model are derived empirically for different mixing strength and fuel type [15]. The model inputs are carbon number and equivalence ratio in the combustion zone. The carbon number is 10 (diesel combustion) for volatiles and the equivalence ratio is calculated based on the actual air flow and air demand.

## 3.0 RESULTS AND DISCUSSION

All the numerical results on the CO-NO pollutant characteristics are presented in Figures 5 to 8. Transversal profiles of gas-phase CO-NO were obtained from the simulations at axial distances 56 mm (z/D=0.2), 112 mm (z/D=0.4), 168 mm (z/D=0.6) and 224 mm (z/D=0.8) from the swirler throat exit position. In total, four radial swirler produced flames were investigated using four swirlers, producing swirl numbers of 0.366, 0.630, 0.978 and 1.427.

Transversal profiles of total carbon monoxide (CO) population in the liquid fuel combustor were obtained similar from the temperature analysis. The CO population was found to be high for low swirl combustion compared with high swirl combustion as seen in Figure 5 and Figure 6. For high swirl flow, the CO population stabilized at short distance from the swirler throat (for SN=1.427 stabilizes at z/D=0.4). For low swirl combustion, the CO population continues to increase from the swirler throat at an average rate of 20% for every z/D of 0.2. It had not stabilized even at z/D=0.8. This was calculated from the area below the graphs at each station in Figures 5a to 5d.

These phenomena could be explained by the presence of the swirl immediately after the swirl throat and the central internal recirculation zone at the core of the chamber. These two physical phenomena helped to quicken the completion of combustion, by the fact that the mixing of fuel is more thorough, and the re-introduction of hot species from the initial combustion zone into the combustion core due to recirculation.

Transversal profiles of total pollutant nitrogen oxide (NO) population in the liquid fuel combustor were obtained from the temperature analysis (Figure 7). The pollutant NO population was found to be well distributed across the combustor for high swirl flow but for low swirl flow this pollutants are more concentrated at the core (SN= 0.978 after z/D=0.6 and for SN=0.366 after z/D=0.8). This correlates with the flame intensity positions, where that intense heat would produce more pollutant NO [14]. In addition, for SN=0.366 the pollutant NO concentration at the combustor core near the swirler throat is very low, which can be explained by the fact that there is no flame at that point. Due to buoyancy, the flame really started at z/D=0.4, after which point the concentration pollutant NO at the core starts to increase.

From Figures 7 and 8, the pollutant NO rate of increase in concentration for high swirl flows (SN=0.978 and 1.427) start at 50% from z/D=0.2 to 0.4, and continued at same rate to z/D=0.6. There after the concentration stabilizes, which means there was no more production of pollutant NO after z/D=0.6. For the low swirl flow, the pollutant NO concentration was very low at positions near the swirler throat and did not increase until z/D=0.6. From this point to z/D=0.8 the concentration increased by 40% and continued increase by 80% up to z/D=1.0.

It should be noted here that the high swirl flows produce wide flames covering the whole of the can cross section, resulting in flames without intense temperature point. This prevents the formation pollutants NO due to high temperatures. For low swirl flows, the flame is more concentrated at the core of the can, away from the swirler throat. This resulted in high temperature intensity zone, which encouraged the formation of thermal pollutant NO. These results point to the importance of elimination of flame peak temperatures from combustors using high swirl flows would reduce the production of pollutant NO.

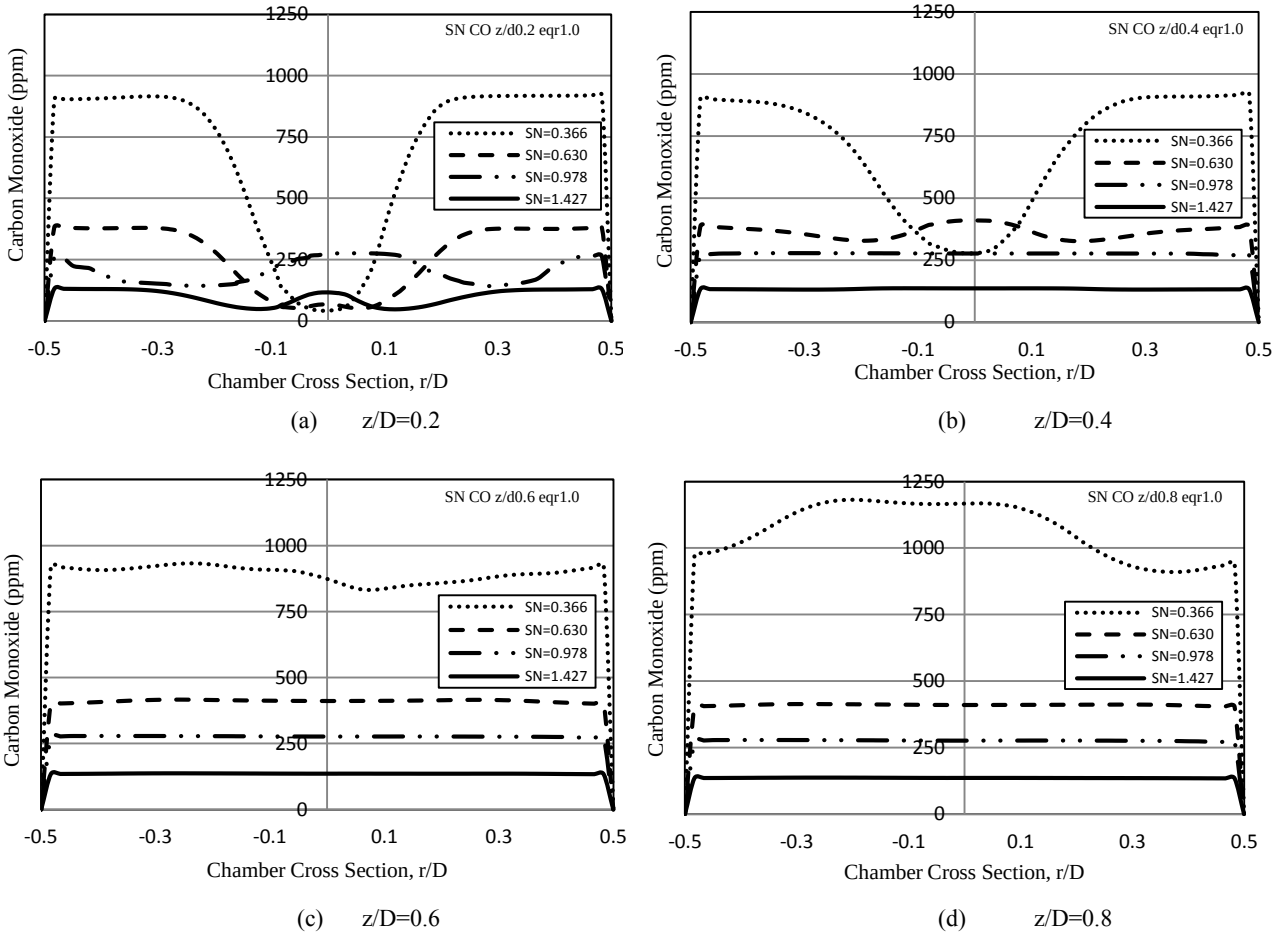


**Figure 5** Transversal profiles of total carbon monoxide at different axial station

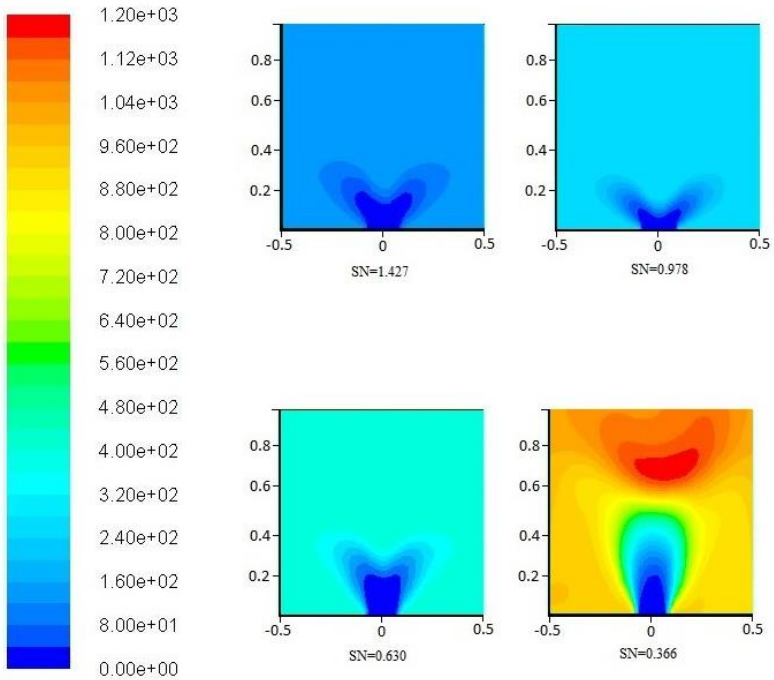


**Figure 6** Total Carbon Monoxide (CO) Contour in Axial Section of the Combustor (Scale is in ppm)

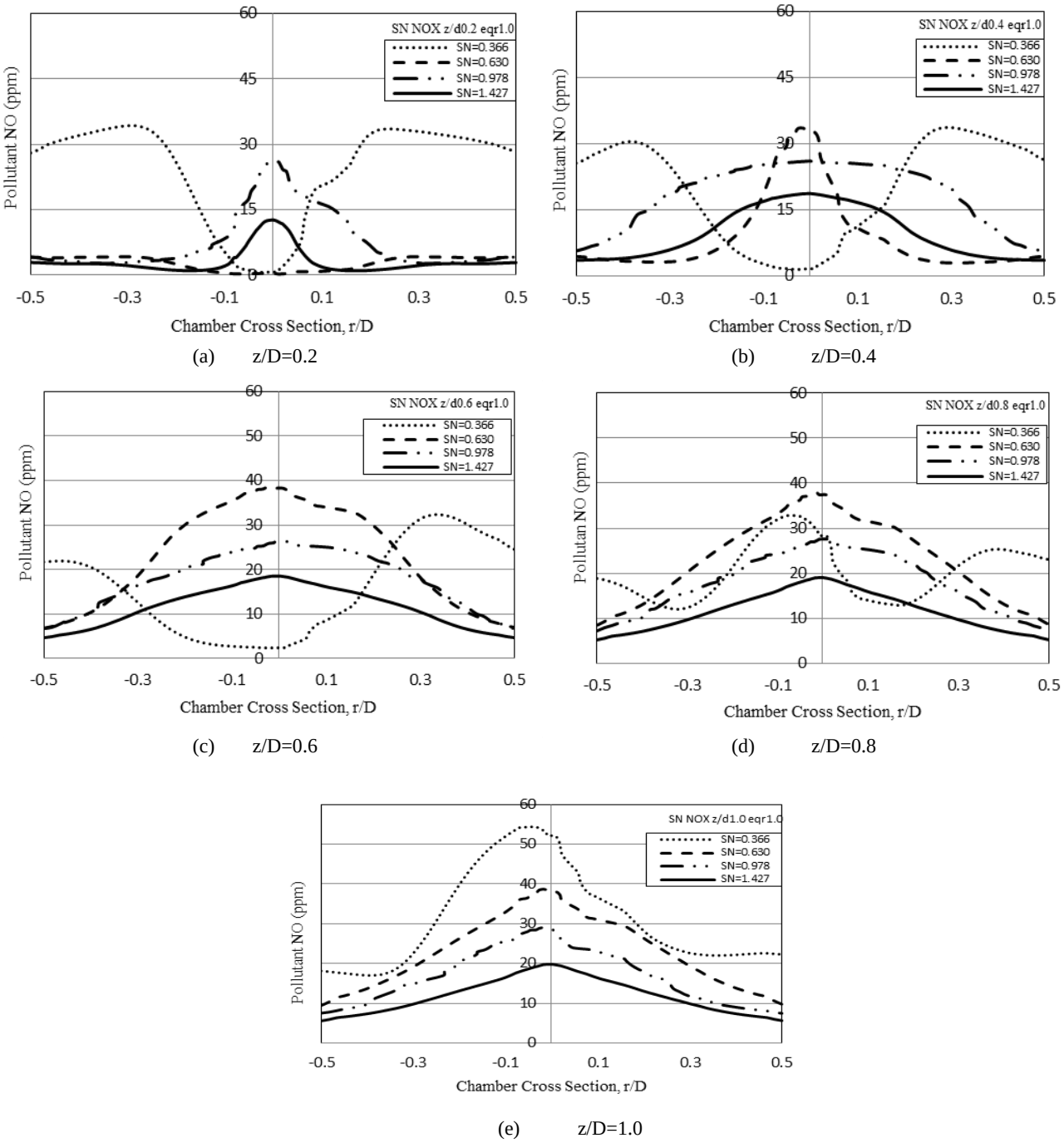


**Figure 7** Transversal profiles of total NO Pollutant at different axial station

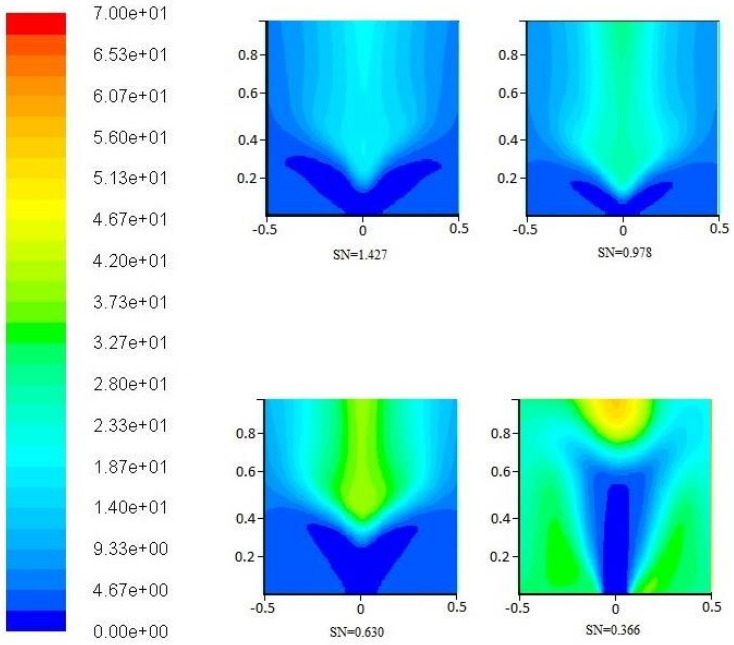


**Figure 8** Total Pollutant Nitrogen Oxide (NO) Contour in Axial Section of the Combustor (Scale is in ppm)

## ■4.0 CONCLUSION

The CFD simulation described in this paper proves that the formation of CO-NO near burner throat in swirling flow combustion system is related to the swirler number/swirler angle. High swirler number produces short but wide flame, and this reduces the time and distance for burning. Besides, it also reduces the peak temperature of the flame, which prevented the formation of pollutant NO. Moreover, high swirler number also leads to the well distributed temperature distribution in the combustor cross section. Because of all these factors, the formation of CO-NO near burner throat is reduced. Therefore, for the future works in the development of an efficient combustion system, the relationship between the swirler number/swirler angle and the formation of CO-NO must be taken into consideration.

## Acknowledgement

The authors would like to thank the Ministry of Higher Education of Malaysia (project number: MTUN-COE 9016-00003) for awarding a research grant to undertake this project. The authors would also like to thank the Faculty of Mechanical Engineering, Universiti Teknologi Malaysia for providing the research facilities and space to undertake this work.

## References

[1] Mathur, D. L. 1974. A New Design of Vanes for Swirl Generation. *IE (I) Journal Me*. 55: 93–96.
[2] Fricker, N. and Leuckel, W. 1976. The Characteristic of Swirl Stabilized Natural Gas Flame Part 3: The Effect of Swirl and Burner Mouth Geometry on Flame Stability. *J. Inst. Furl*. 49: 152–158.
[3] Mestre, A and Benoit, A. 1973. Combustion in Swirling Flow. *14th Symposium (International) on Combustion, The Combustion Institute.* Pittersburg. 719.
[4] Chervinskey, A. and Manheimertiment, Y. 1968. Effect of Swirl on Flame Stabilization. *Israel Journal of Technology*. 6(2): 25–31.
[5] Tian, Z. F., Witt, P. J., Schwarz, M. P., & Yang, W. 2010. Numerical Modelling of Victorian Brown Coal Combustion in a Tangentially Fired Furnace. *Energy & Fuels*. 24(9): 4971–4979.
[6] Khalil, K. H., El-Mehallawy, F. M. and Moneib, H. A. 1977. Effect of Combustion Air Swirl on the Flow Pattern in a Cylindrical Oil Fired Furnace, *16th Symposium (International) on Combustion, The Combustion Institute, Pittersburg*. 135–143.
[7] Apack, G. 1974. Interaction of Gaseous Multiple Swirling Flames. Phd Thesis. Department of Chemical Engineering and Fuel Technology, University of Sheffield.
[8] Gupta, A. K., Lilley, D. G. and Syred. 1984. N. *Swirl Flows.* Abacus Press, Tunbridge Wells, England.
[9] Chen R. H. and Driscoll J. F. 1988. The Role of the Recirculation Vortex in Improving Fuel-air Mixing within Swirling Flames. *22nd Symposium (International) on Combustion*. The Combustion Institute, Pittsburgh. 531–54.
[10] Beer, J. M., Chigier, N. A. 1972. *Combustion Aerodynamics*. Applied Science Publisher, London.
[11] Kim, Y. M., Chung, T. J. 1989. Finite- Element Analysis of Turbulent Diffusion Flames. *AIAA J.* 27(3): 330–339.
[12] Versteeg, H. K., Malalasakera, W. 1995. *An Introduction to Computational Fluid Dynamics, the Finite Volume Method*. Longman Group Ltd.
[13] FLUENT 14.0 User's Guide, Fluent Inc. 2012.
[14] King, P. T., Andrews, G. E., Pourkashanian, M. M., & McIntosh, A. C. 2012. Nitric Oxide Predictions for Low NOx Radial Swirlers With Central Fuel Injection Using CFD. In ASME Turbo Expo 2012: Turbine Technical Conference and Exposition American Society of Mechanical Engineers. 985–993.
[15] Zhou, W., Moyeda, D., Payne, R., & Berg, M. 2009. Application of numerical simulation and full scale testing for modeling low NOX burner emissions. *Combustion Theory and Modelling*. 13(6): 1053–1070.